Design and fabrication of integrated optical elements in glasses and crystals by various ion beam techniques

I. Bányász[1*], S. Pelli[2,3], G. Nunzi-Conti[2], G. C. Righini[3], S. Berneschi [2], E. Szilágyi[1], A. Németh[1], M. Fried[4], T. Lohner[4], P. Petrik[4], Z. Zolnai[4], N.Q. Khanh[4], . Rajta[5], G.U.L. Nagy[5], V. Havranek[6], V. Vosecek[6], V. Lavrentiev[6], M. Veres[7], L. Himics[7]

[1]Department of Nuclear Materials Science, Wigner Research Centre for Physics, Hungarian Academy of Sciences, P.O.B. 49, H-1525, Budapest, Hungary

[2]MDF-Lab, "Nello Carrara" Institute of Applied Physics, IFAC-CNR, Via Madonna del Piano 10, 50019 Sesto Fiorentino (FI), Italy

[3] "Enrico Fermi" Center for Study and Research, Piazza del Viminale 2, 00184 Roma, Italy

[4]Research Institute for Technical Physics and Materials Science, Centre for Energy Research, Hungarian Academy of Sciences, Budapest, P.O.B. 49, H-1525 Hungary

[5]MTA Atomki, Institute for Nuclear Research, Hungarian Academy of Sciences, H-4001 Debrecen, P.O. Box 51, Hungary

[6]Nuclear Physics Institute AV CR, Řež near Prague, 250 68, Czech Republic

[7]Department of Applied and Nonlinear Optics, Wigner Research Centre for Physics, Hungarian Academy of Sciences, P.O.B. 49, H-1525, Budapest, Hungary

Abstract

Researches were initiated on ion beam fabrication of planar and channel optical waveguides in tellurite glasses. Channel waveguides were written in Er: TeO_2WO_3 glass through a special silicon mask using 1.5 MeV N^+ irradiation. This method was improved by increasing N^+ energy to 3.5 MeV to achieve confinement at the 1550 nm wavelength, too. An alternative method, direct writing of the channel waveguides in the tellurite glass using focused beams of 6–11 MeV C^{3+} and C^{5+} as

* Corresponding author. Tel.: +36 1 392 2222x1732; fax: +36 1 392 2215.
E-mail address: banyasz.istvan@wigner.mta.hu (I. Bányász).

well as 5 and 10 MeV N^{3+} and N^{4+}, has also been developed. Besides of planar waveguides, channel waveguides were also fabricated in undoped eulytine ($Bi_4Ge_3O_{12}$) and sillenite type ($Bi_{12}GeO_{20}$) bismuth germanate crystals using both a special silicon mask and a thick AZ4562 photoresist mask and 3.5 MeV N^+ irradiation. The waveguides were studied by various techniques, such as phase contrast, interference contrast and interference phase contrast microscopies, atomic force microscopy, surface profilometry, micro Raman spectroscopy. Guiding properties were checked by using m-line spectroscopy and end fire coupling method.

1. Introduction

Active and passive optical waveguides and optical gratings are fundamental elements in modern telecommunications systems. A large number of optical crystals and glasses were identified and are used as suitable optoelectronic materials. However, fabrication of waveguides in some of these materials remains still a challenging task due to their susceptibility to mechanical or chemical damages during processing. Ion beam implantation is able to modify the optical properties of optical materials, such as some polymers, glasses and crystalline materials. Numerous practical applications exist, e.g. waveguides, special coatings, optical confinement of semiconductor lasers, impurity additions for lasing regions, fabrication of nonlinear optical elements, and production of photochromic layers (in optical disks) [1-4]. The first ion implanted waveguides were produced by Schineller *et al*. by proton implantation into fused silica glass in 1968 [5].

Light ions like H and He of relatively low energies were used for the implantation of the optical waveguides from the beginning until recently [6 – 10]. Medium- and higher mass ions were also used to modify optical properties of materials, like Li^+, B^+, Na^+, Ar^+, Bi^+ by Webb and Townsend [11].

Besides H^+ and He^+, Ar^+ ion implantation was also used by Mazzoldi [12]. Various medium-mass ions, especially carbon and oxygen, were used for fabrication of optical waveguides in amorphous and crystalline materials [13 – 17].

Formation of adequate refractive index changes for waveguide fabrication requires relatively high fluences, in the 10^{15} -10^{17} ions/cm^2 region, especially when the mass and energy of the

implanting ion are low. Chen and co-workers reported successful planar waveguide formation in Nd: YVO_4 crystal by 3.0 MeV Si^+ ion implantation at a relatively low fluence of $1 \cdot x\ 10^{15}$ ions/cm^2 [18]. They attributed the lower formation of a refractive index barrier to the nuclear interaction of the implanting ion with the target, while the slight refractive index increases in the guiding region to the electronic interaction. Vázquez and her co-authors used 7-MeV C^{2+} ions of a fluence of $1 \cdot 10^{16}$ ions/cm^2 to produce planar optical waveguides in Nd: YAG crystal [19]. They attributed the waveguide formation to a similar mechanism like Chen *et al.* They claimed that the use of group IV elements such as carbon leads to distortions, which are not localized at a single site, but influence some tens of nearby lattice atoms. Defect retention is induced via defect trapping at the perturbed sites. As carbon is chemically active, there could be a series of defect models such as carbide bonds, carbonate groups, etc. [20].

First studies on the effects of swift heavy ion irradiation on the optical properties of materials date back to the 1990's. Aithal and his co-workers irradiated organic nonlinear optical crystals with 100 MeV Ag^{14+} ions, and studied optical properties of the irradiated samples [21]. They claimed that their results opened a possible method of fabricating optical waveguides in such organic nonlinear optical crystals. Opferman *et al*. detected formation of amorphous tracks and layers in $KTiOPO_4$ crystals during implantation with swift heavy ions at low fluences (150 MeV Kr and 250 MeV Xe, $3 \cdot\bullet\ 10^{12}$ ions/cm^2 - $4 \cdot\ 10^{13}$ ions/cm^2) [22]. Track and amorphous layer formation were due to electronic interaction, and could be explained using the Gibbons model [23]. Bentini et *al.* performed a systematic study of the effects of implantation with medium-light elements, N, O and F, of 4 – 5 MeV energies and of $1 \cdot\ 10^{14}$ ions/cm^2 - $6 \cdot\ 10^{14}$ ions/cm^2 fluences of $LiNbO_3$ crystals [24]. They concluded that the mechanism governing the damage formation is strongly connected to the Z number of the implanted ions and to the interaction of defects produced by electronic interactions. Olivares *et al*. implanted $LiNbO_3$ crystals using 5-MeV Si^{2+}, 7.5-MeV Si^{2+} and 30-MeV Si^{5+} ions with fluences from $5 \cdot 10^{13}$ ions/cm^2 - $1 \cdot\ 10^{15}$ ions/cm^2 [25]. Optically isotropic amorphous layers of thicknesses increasing with fluence were produced. The same group succeeded in fabricating planar optical waveguides in $LiNbO_3$ crystals via implantation with 20- and 22-MeV fluorine ions and fluences from $1 \cdot\ 10^{14}$ ions/cm^2 - $3 \cdot 10^{15}$ ions/cm^2 [26]. Amorphised layer situated around the maximum of electronic stopping power served as optical barriers while the layer left below the crystal surface remained crystalline and constituted the well of the optical waveguide.

Fabrication of optical gratings is also among the possible optical applications of ion implantation [27]. Previous experiments showed that during ion implantation, a surface structure may also appear due to the induced volume change, resulting in mixed-type (surface relief and index of refraction) gratings [27, 28]. Rajta *et al*. investigated the refractive index depth profile in PMMA due to proton irradiation, and found that the highest increase of the refractive index occurs at the end-of-range (Bragg-peak) of the penetrating protons [29]. This allows us to produce diffractive optical elements by modulating the refractive index of the material well below its surface by use of high energy ion implantation. Successful realization of fine transmission optical gratings of high diffraction efficiency in glass via irradiation with MeV-energy He^+ and N^+ ions through thick photoresist mask was reported in 2001 [27]. Since the development of ion microbeam facilities attached to accelerators, proton microbeams have been extensively used for producing gratings and other microoptical elements in organic and inorganic optical materials [30].

We present our recent results in the following areas: Design and fabrication of planar waveguides in optical crystals and glasses using implantation of nitrogen ions. Ion energies ranged from 1.5 MeV to 3.5 MeV, fluences were between $1 \cdot 10^{14}$ ions/cm^2 and $8 \cdot 10^{16}$ ions/cm^2. Target materials were Er: TeO_2WO_3 glass (Er-Te glass), Pyrex glass and both eulytine and sillenite type bismuth germanate (BGO). Composition of the Er-Te glass used for our experiments was 60 TeO_2-25 WO_3-15 Na_2O-0.5 Er_2O_3 (mol. %). Both single energy and multi energy implantations were performed. Guiding properties were improved by thermally annealing the implanted Design and fabrication of channel waveguides in optical crystals and glasses using implantation of nitrogen and carbon ions. Both masking techniques and direct writing using ion microbeams were used. Nitrogen and carbon ions were used for the implantations in the energy range of 1.5 MeV - 11 MeV, fluences were between $1 \cdot 10^{14}$ ions/cm^2 and $8 \cdot 10^{16}$ ions/cm^2.

2. Experimental

2.1 Design of the optical elements

Main physical parameters of the optical elements to be fabricated via ion implantation can be determined by simulations using the SRIM (Stopping and Range of Ions in Matter) code [31]. Ion species and energy have to be chosen according to the desired thickness of the optical element.

Depth distributions of the implanted ions in the sample give good approximations for the structure of the waveguides if nuclear interaction is the dominant one. In case of swift heavy ions, it is the ionisation *vs.* depth distribution which can be used for the prediction of the waveguide structure.

Results obtained for the Er-Te glass are shown in Fig. 1. Irradiation with N^+ ions of 1.5-MeV energy gives a projected range of ions of 1.5 μm with a longitudinal straggling of 0.2 μm. By increasing the N^+ ion energy to 3.5 MeV, one obtains 2.5 μm for the range and 0.3 μm for the longitudinal straggling. When setting the N^{3+} ion energy to 5 MeV, the projected range increases to 3.1 μm and the longitudinal straggling is 0.3 μm. Irradiation with 6.027-MeV C^{3+} ions yields a projected range of 4.0 μm and a longitudinal straggling of 0.3 μm. Finally, when using C^{4+} ions of 11.04 MeV energy, the projected range and longitudinal straggling increase to 6.8 μm and 0.4 μm, respectively.

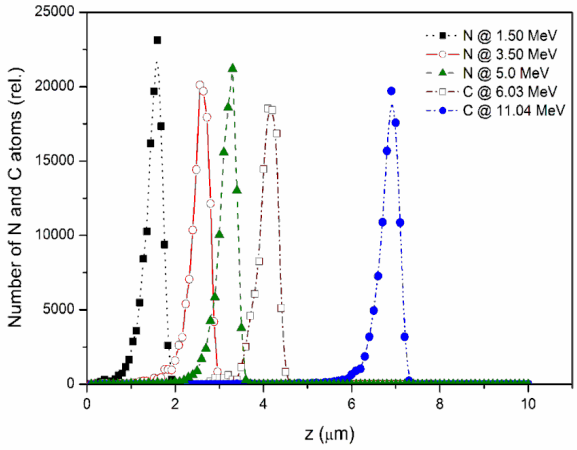

Figure 1. Depth-distributions of the implanted nitrogen and carbon ions in Er: Tungsten – Tellurite glass. Ion species and energy are indicated in the legend.

Distributions of implanted nitrogen ions in sillenite type BGO crystal ($Bi_{12}GeO_{20}$) are presented in Fig. 2. This material is of very high density, and stopping ranges of nitrogen ions in it are lower than those in Er: Tungsten – Tellurite glass. Consequently, the expected waveguide thicknesses are also smaller.

When medium mass ions of considerably higher energy are implanted in the target, electronic interaction becomes the dominant one. There is a consensus that ions can be considered Swift Heavy Ions (SHI) when their energy is above 1 MeV/amu. Formation of an amorphised layer around the maximum of the electronic stopping power even at very low fluences (below 10^{12} ions/cm^2) can be expected [32]. In our experiments the highest ion energies are around the above limit, so the results are interesting also

from a theoretical point of view. Our experiments are novel also in a sense that SHI implantation has not been used for optical element fabrication in amorphous materials (glasses).

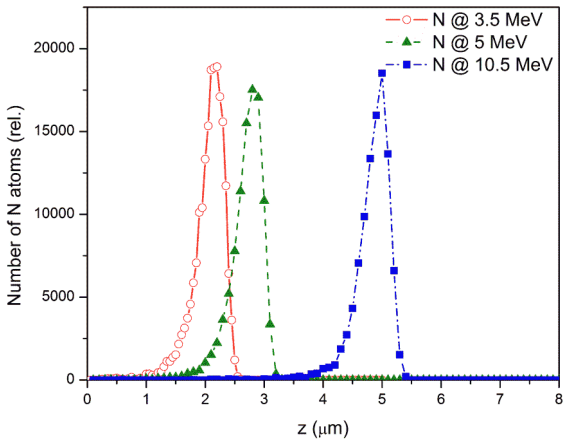

Figure 2. Depth-distributions of the implanted nitrogen ions in sillenite type BGO crystal.

2.2 Fabrication of the optical elements

Nitrogen ion implanted planar waveguides in Er-Te glass and eulytine and sillenite type BGO crystals were fabricated at the van de Graaff accelerator of the Wigner Research Centre for Physics, Budapest at energies of 1.5 MeV and 3.5 MeV. In some cases, multi-energy implantation was applied to increase the barrier thickness and thus suppress or reduce leaky modes in the waveguides. The fluences ranged in the $10^{14} – 10^{17}$ ions/cm^2 interval.

Three methods were applied to the fabrication of channel waveguides in Er-Te glass and eulytine and sillenite type BGO crystals. The first one was implantation through a special silicon membrane mask that contained 24 μm wide slits. The second method was patterning an 8 μm thick AZ4562 photoresist layer on the surface of the sample. The photoresist was processed to obtain trapezoidal line profiles to facilitate waveguide side wall formation when the samples were implanted through it. The thickness of the channel waveguides was between 5 μm and 15 μm. A SEM image of a detail of the used photoresist layer is shown in Fig. 3.

Experiments using both methods were also carried out at the van de Graaff accelerator of the Wigner Research Centre for Physics, using N ions at energies of 1.5 MeV and 3.5 MeV. The third method was direct the writing of 15-μm wide channel waveguides in Er-Te glass with carbon and nitrogen microbeams of low (5 MeV and 6.027 MeV) and high (10.5 MeV and 11.04 MeV) energy using a 3-MV Tandetron 4130 MC (High Voltage Engineering Europa B.V.) accelerator with a quadrupole triplet OM150 Oxford Microbeams Ltd. at the Řež Nuclear Physics Institute, Czech Republic.

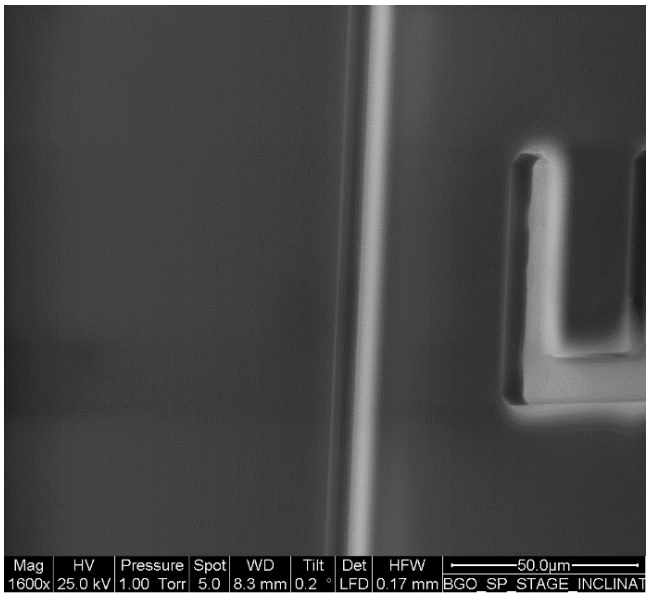

Figure 3. SEM image of an aperture in the AZ4562 photoresist mask for selective N^+ irradiation of a BGO sample. The intended trapezoidal shape of the walls of the aperture is evident.

3. Results

3.1 Optical microscopy

Ion implanted planar and channel optical waveguides and index-of-refraction and surface relief or mixed transmission optical gratings are generally phase objects. Thus, they are hardly visible by standard optical microscopy (by conventional optical microscopy only the implantation induced absorption changes and surface damage can be seen). Phase objects can be observed using interference- , phase contrast- and interference phase contrast (INTERPHAKO)-microscopy. Modulations of the optical path through the phase object are visualised as deformations of a parallel and equidistant interference fringe system in interference microscopy. Optical path modulations are mapped into (virtual) absorption variations in phase contrast microscopy. The INTERPHAKO method visualises optical path variations as changes in the hue of interference colours on the object.

INTERPHAKO microscopic image of the corner of an N ion implanted planar waveguide are shown in Fig. 4.

Reflection INTERPHAKO microscopic images of channel waveguides, implanted also with N^+ ions at E = 1.5 MeV and various fluences, are presented in Fig. 5.

Dependence of the induced refractive index change on the implanted fluence can clearly be seen by the increasing contrast of the waveguides in Fig. 5 a) through d), since increasing contrast of hue indicates increasing modulation of the optical path.

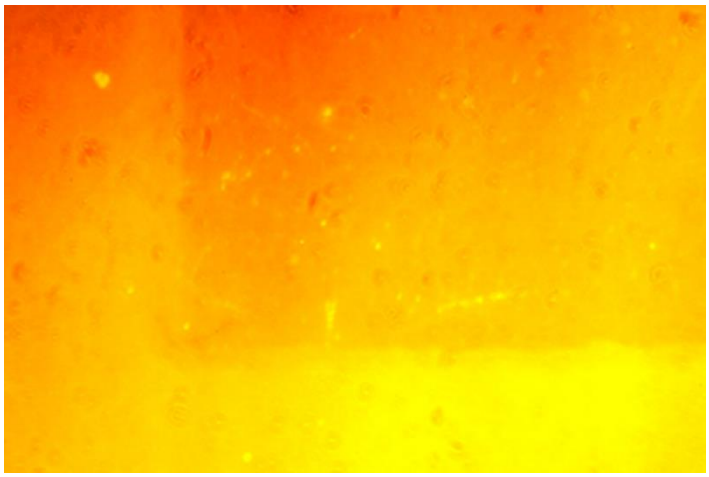

Figure 4. INTERPHAKO microscopic image of the corner of an ion implanted planar optical waveguide. The material is Er-Te glass; Implantation: N^+ ions, E = 1.5 MeV, Fluence = $8 \cdot 10^{16}$ ions/cm^2; Zeiss Peraval microscope; Objective: 6.3 X; Ringblende: 6.3 X, taken in transmission.

Interference- and phase contrast microphotographs of channel waveguides fabricated in eulytine and sillenite type BGO crystals using the same method are presented in Fig. 6. The fluences were $2 \cdot 10^{15}$ ions/cm^2 (A) and $1 \cdot 10^{15}$ ions/cm^2 (B). The magnifications were 500 x and 250 x. Similar results were obtained as with the waveguides fabricated in Er-Te glass.

Phase contrast microscopic images of three channel waveguides fabricated in Er-Te glass, using a 15 μm wide microbeam of 5.0 MeV N^{3+} ions are presented in Fig. 7. The fluences were $0.5 \cdot 10^{15}$ ions/cm^2 (A), $1 \cdot 10^{16}$ ions/cm^2 (B) and $2 \cdot 10^{16}$ ions/cm^2 (C). One can see the large difference in the irradiation-induced refractive index change.

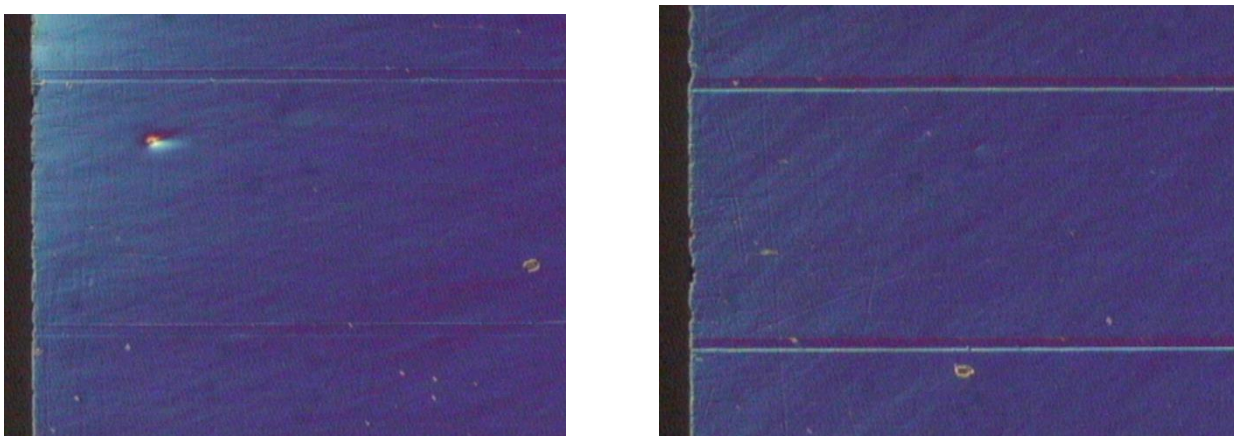

Figure 5. INTERPHAKO microscopic image of two channel waveguides implanted in Er-Te glass using the silicon mask, N^+ ions, energy of 1.5 MeV and a fluence of **a)** $2 \cdot 10^{15}$ ions/cm^2 and **b)** $4 \cdot 10^{15}$ ions/cm^2.

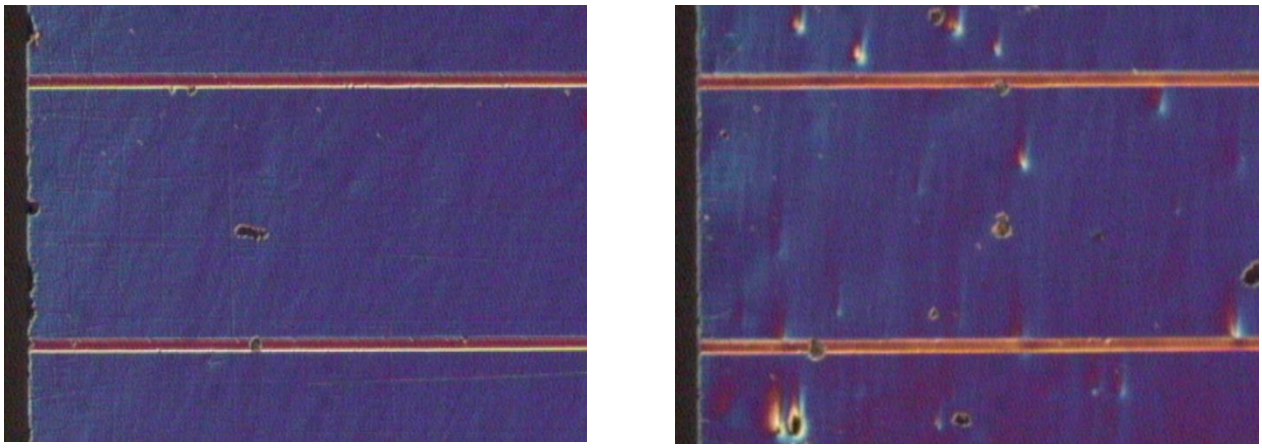

Figure 5. cont. INTERPHAKO microscopic image of two channel waveguides implanted in Er-Te glass using the silicon mask, N^+ ions, energy of 1.5 MeV and a fluence of **c)** $6 \cdot 10^{15}$ ions/cm^2 and **d)** $8 \cdot 10^{15}$ ions/cm^2.

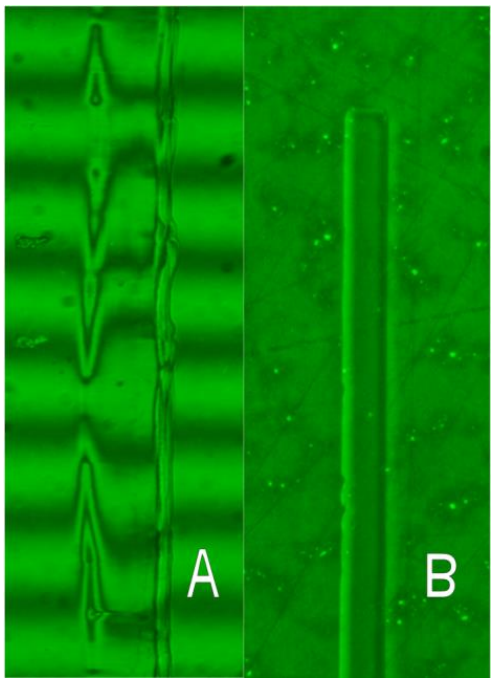

Figure 6. Interference- and phase contrast microscopic images of channel waveguides fabricated in eulytine (A) and sillenite (B) type BGO crystals using a 3.5-MeV N^+ irradiation through a silicon mask. The fluences were $2 \cdot 10^{15}$ ions/cm^2 and $1 \cdot 10^{15}$ ions/cm^2, respectively.

3.2 Other techniques

Transmission microscopies presented in the previous section give only the lateral distribution of the full optical path variation across the sample. Especially in the case of optical waveguides, the knowledge of the depth distribution of refractive index is crucial in assessing the functionality of the waveguide. Spectroscopic ellipsometry (SE) was used to determine those parameters of the ion implanted planar optical waveguides [33]. Measurements were performed with a Woollam M-2000DI spectroscopic ellipsometer (wavelength range of 193-1690 nm), except for the 1.5 MeV N^+ irradiated Er: Te glass samples, where a SOPRA ES4G ellipsometer was used in the in the wavelength range of 400 -1000 nm. Examples of the results of SE measurements and simulations are shown in Table 1 and Fig. 8.

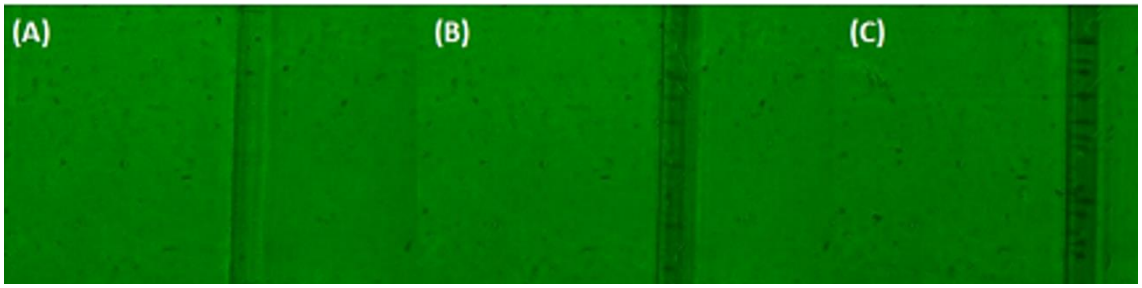

Figure 7. Phase contrast microscopic image of three channel waveguides fabricated using a 15 μm wide microbeam of 5.0-MeV N^{3+} ions. The N^{3+} ion fluences were $0.5 \cdot 10^{16}$ ions/cm^2 (A), $1 \cdot 10^{16}$ ions/cm^2 (B) and $2 \cdot 10^{16}$ ions/cm^2 (C).

Measurements were performed with a Woollam M-2000DI spectroscopic ellipsometer (wavelength range of 193-1690 nm), except for the 1.5 MeV N^+ irradiated Er: Te glass samples, where a SOPRA ES4G ellipsometer was used in the in the wavelength range of 400 -1000 nm. Examples of the results of SE measurements and simulations are shown in Table 1 and Fig. 8.

N^+ energy (MeV)	1.5				3.5			
Names of the waveguides	E	F	G	H	A	B	C	D
Fluences (x10^{16} ions/cm^2)	1	2	4	8	1	2	4	8
Thickness of layer$_2$ [nm]	1781 ± 19	1785 ± 28	1779 ± 16	-	2615.1 ± 1.6	2643.6 ± 14.5	2403.8 ± 5.1	2384.7 ± 4.6
Refractive index of layer$_2$ at 635 nm	2.052	2.048	2.052	-	2.063	2.042	2.040	2.097
Refractive index of layer$_2$ at 1550 nm					1.984	1.965	1.969	1.962
Thickness of layer$_1$ [nm]	67 ± 22	83 ± 35	97 ± 19	-	183.4 ± 9.8	195.8 ± 4.6	457.3 ± 4.7	489.8 ± 8.6
Refractive index of layer$_1$ at 635 nm	2.071	2.068	2.071	-	2.014	2.025	2.070	2.004
Refractive index of layer$_1$ at 1550 nm					1.954	1.955	1.936	1.960
Refractive index of the non-implanted glass at 635 nm	2.081	2.081	2.081	-	2.019	2.019	2.019	2.019
Refractive index of the non-implanted glass at 1550 nm					1.950	1.950	1.950	1.950

Table 1. Results of SE measurements of ion implanted Er: tellurite glass waveguides

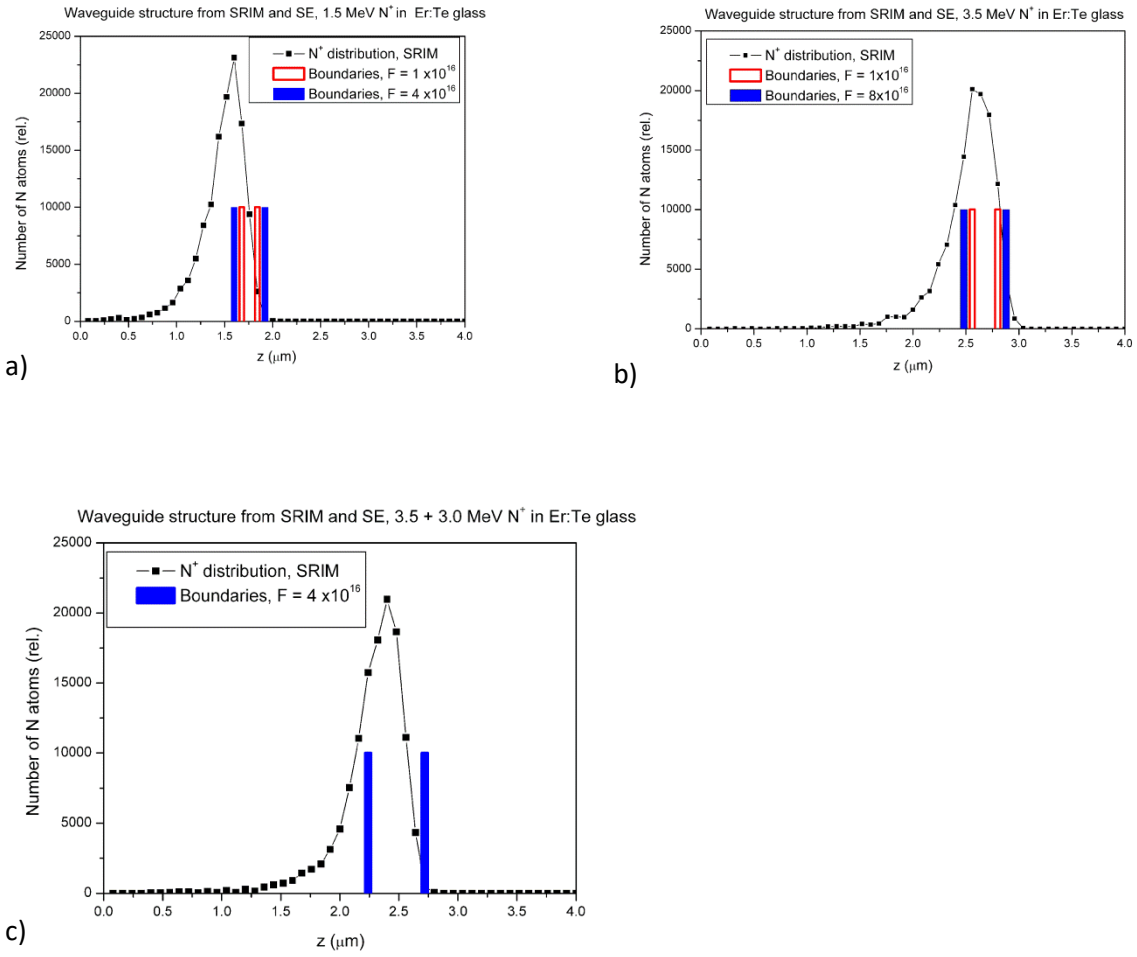

Figure 8. SRIM simulation and SE fit of the waveguide structure in Er: Te glass at various irradiation energies and fluences: a) E = 1.5 MeV, fluences are 1 $\cdot 10^{16}$ and 4 $\cdot 10^{16}$. b) E = 3.5 MeV, fluences are 1 $\cdot 10^{16}$ ions/cm^2 and 8 $\cdot 10^{16}$ ions/cm^2. c) E = 3.5 MeV + 3.0 MeV, fluence is 4 $\cdot 10^{16}$ ions/cm^2.

SE measurements and simulations locate the barrier layers close to the maximum of the distribution of the implanted N^+ ions, predicted by SRIM simulations. As expected, higher fluences result in wider barrier layers (Figs. 8 a) and b**)**). While single energy implantation produces a barrier thickness of 300 nm, double energy implantation at the same total fluence gives a barrier thickness of about 650 nm.

Micro Raman spectroscopy was also used to study the structure of the channel waveguides and optical gratings fabricated by ion implantation. The very promising preliminary results show

significant differences between the non-irradiated sample and the waveguides, as it can be seen in Fig. 9. In this figure, new Raman peaks appear in the spectrum in the implanted region, when working in the red (λ = 670 nm).

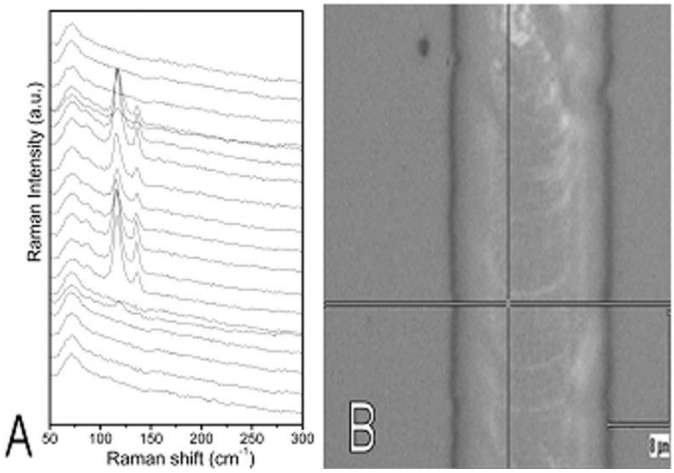

Figure 9. Micro Raman spectra (A) taken across a channel waveguide (B) fabricated in an Er-Te glass with 3.5 MeV N^+ ion implantation through a silicon mask). The parameter of the vertically shifted curves is the laser microbeam position along the horizontal line in the microphotograph.

3.3 M-line spectroscopy and channel waveguide tests

COMPASSO, a semi-automatic m-line spectroscopic instrument, developed at IFAC, was used for the characterization of the planar waveguides implanted in the samples. The availability of m-line spectroscopic data at several wavelengths (635, 980, 1310 and 1550 nm) has allowed us to obtain a more accurate and flexible data processing. Actually, assuming a Sellmeier-like law to account for chromatic dispersion for all layers:

$$n^2 = 1 + \frac{\lambda^2}{A\lambda^2 + B}, \qquad (1)$$

and using it in the fit process, it was possible to obtain the thickness of the guiding layer and the parameters A and B for the guiding and the barrier layers in a broad wavelength range. As shown in Fig. 11, for the sample irradiated with N^+ ions of 3.5-MeV energy and a fluence of $4 \cdot 10^{16}$ ions/cm^2 , the fit process allowed us to model the wavelength dependent refractive index through parameters *A* and *B* of both the guiding (nf) and barrier layers (ns). Moreover, the effective indices of the modes were calculated with the values of the numerical regression results

and the same assumptions used in the fit process. The agreement between the experimental data (dots in Fig. 10) and the calculated effective indices is very good. The thickness of the guiding layer was assessed to be 2.2 μm, in agreement with the SRIM simulations.

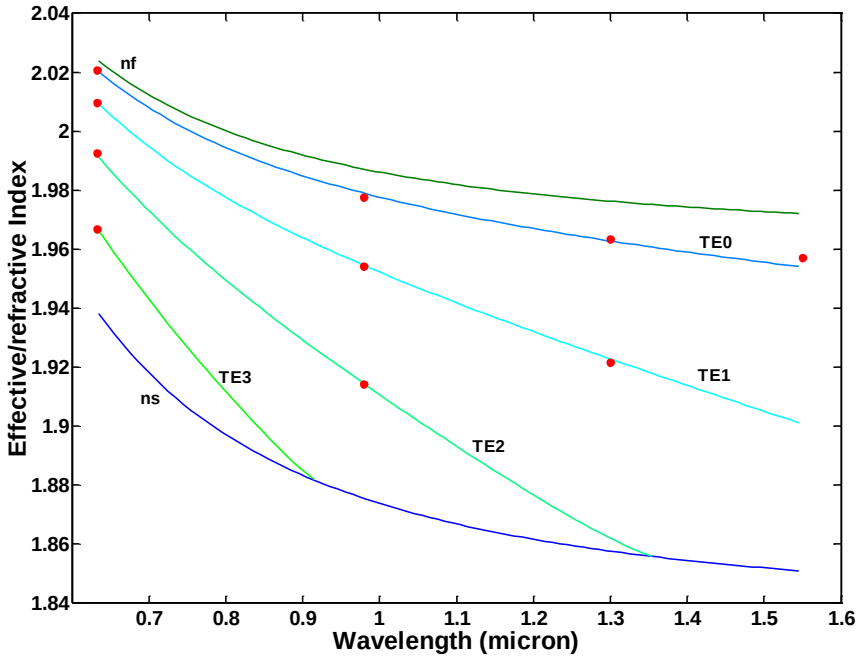

Figure 10. Reconstruction of the refractive index of the guiding (nf) and barrier layer (ns) as a function of the wavelength. Sample irradiated with $4 \cdot 0^{16}$ ions/cm^2. Experimental effective indices of the modes are also shown (red dots).

Channel waveguides were tested for functionality by the end-fire method. The guiding has been confirmed only in the 1.5 MeV N^+ ion implanted Er-Te waveguides so far, up to 980 nm. Results of preliminary tests show that channel waveguides fabricated in eulytine and sillenite BGO crystals, using the silicon mask and 3.5 MeV N^+ ion implantation, worked up to $\lambda = 1530$ nm. A proof of the functionality of such a waveguide is shown in Fig. 11. Operation at $\lambda = 1530$ nm of channel waveguides written in Er-Te glass samples with focused ion beam of 11 MeV C^{5+} was also observed. Propagation losses of the so far tested as-implanted channel waveguides range from 7 to 15 dB/cm. After all the as-implanted waveguides will have been tested, adequate thermal annealing will be applied to them, and functionality test will be repeated. According to previous experience, thermal annealing can reduce propagation losses by a factor of 10.

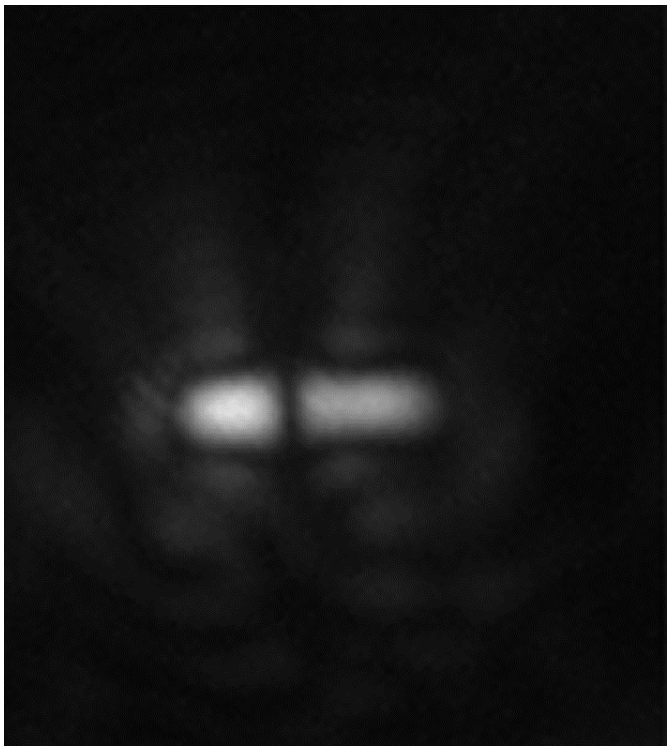

Figure 11. Microscopic image of the guided wave (first-order mode) emerging from the output face of a channel waveguide fabricated in eulytine BGO via 3.5 MeV N^+ implantation at a fluence of 10^{16} ions/cm^2 through silicon mask. λ = 1530 nm.

4. Conclusion

A review of researches on the design and fabrication of planar and channel waveguides and optical gratings in optical glasses and crystals, using implantation of various ions at relatively wide ranges of energy and fluence is presented. Guiding modes were detected in 3.5 MeV N^+ ion implanted planar waveguides both in Er-Te glass and sillenite type BGO crystals, without post implantation thermal annealing. The waveguides in sillenite type BGO worked only up to 1310 nm. Three methods were proposed and realized for channel waveguide fabrication in glasses and crystals, including implantation through a special silicon mask using 1.5 MeV and 3.5 MeV N^+ implantation. Direct writing of the channel waveguides in the tellurite glass using focused beams of 6–11 MeV C^{3+} and C^{5+} and 5 and 10 MeV N^{3+} and N^{4+} has also been developed. Channel waveguides were formed using a thick AZ4562 photoresist mask and an N^+ irradiation of 3.5 MeV, too. The target materials were Er-Te glass, and eulytine and sillenite type BGO. Channel waveguides fabricated in Er-Te glass with 1.5 MeV implantation proved to work up to the wavelength of 980 nm. Green up-conversion along the channel waveguide was also demonstrated [27]. Preliminary test showed that both low-energy N^+ ion implantation through silicon mask in eulytine and sillenite type BGO crystals and direct writing with high-energy focused C^{5+} ions Er-Te glass produced channel working that worked up to the wavelength of 1530 nm.

Although evaluation of a large part of the ion beam implanted optical elements is still under way, the results so far confirmed show that ion beam fabrication is an adequate method for fabrication of various types of optical elements. The use of swift heavy ions is an especially promising method, since it requires very low fluences (down to 10^{12} ions/cm^2), corresponding to short processing times.

Acknowledgements

This work was supported by the following funds: Hungarian National Research Fund (OTKA) project 101223, TAMOP 4.2.2.A-11/1/KONV-2012-0036 Project, co-financed by the European Union and European Social Fund. Support of the CANAM organization under grant No. LM 2015056 is gratefully acknowledged.

References

[1] Townsend, P. D., Chandler, P. J. and Zhang, L., Optical Effects of Ion Implantation, Cambridge University Press, Cambridge, U.K. (1994)

[2] **Ch**en, F., Wang, Xue-Lin and Wang, Ke-Ming, "Development of ion-implanted optical waveguides in optical materials: A review", Opt. Mat., 29, 1523-1542, DOI: 10.1016/j.optmat.2006.08.001 (2007).

[3] Chen, F., "Micro- and submicrometric waveguiding structures in optical crystals produced by ion beams for photonic applications", Laser Photon. Rev., 6, 622-640 (2012)

[4] Peña-Rodríguez, O., Olivares, J., Carrascosa, M., García-Cabañes, A., Rivera A. and Agulló-López, F., "Optical Waveguides Fabricated by Ion Implantations/Irradiation: A Review", in: Ion Implantation, Prof. Mark Goorsky (Ed.), ISBN: 978-953-51-0634-0, InTech, Available from: http://www.intechopen.com/books/ion-implantations/optical-waveguides-fabricated-by-ion-implantation-irradiation-a-review (2012)

[5] Schineller, E. R., Flam, R. P. and Wilmot, D. W., "Optical Waveguides Formed by Proton Irradiation of Fused Silica", J. Opt. Soc. Am.,58, 1171 (1968)

[6] Destefanis, G. L., Townsend, P. D. and Gaillard, J. P., “Optical waveguides in LiNbO3 formed by ion implantation of helium”, Appl. Phys. Lett., 32, 293 (1978)

[7] Mahdavi S M, Chandler P J and Townsend P D, “Formation of planar waveguides in bismuth germanate by 4He+ ion implantation”, J. Phys. D: Appl. Phys. 22 1354-7 (1989)

[8] V. Petit, P. Moretti, P. Camya, J.-L. Doualan , R. Moncorg, “Active waveguides produced in Yb^{3+}:CaF2 by H^{+} implantation for laser applications”, Journal of Alloys and Compounds, 451, 68–70, (2008)

[9] Yingying Ren, Yang Tan, Feng Chen, Daniel Jaque, Huaijin Zhang, Jiyang Wang, and Qingming Lu, "Optical channel waveguides in Nd:LGS laser crystals produced by proton implantation," Opt. Express,18, 16258-16263 (2010)

[10] Jia, Yuechen and Chen, Feng, “Optical channel waveguides in ZnSe single crystal produced by proton implantation”, OPTICAL MATERIALS EXPRESS, 2, 455-460 (2012)

[11] Webb, A.P. and Townsend, P. D., “Refractive index profiles induced by ion implantation into silica”, J. Phys. D: Appl. Phys. 9, 1343-54 (1976)

[12] Mazzoldi, P., “Properties of ion implanted glasses”, Nuclear Instruments and Methods in Physics Research, 209-2010, Part 2, 1089–1098 (1983)

[13] Tan Y, Chen F: "Experimental observation and numerical simulation of guided modes in Nd : $YLiF_4$ channel waveguides produced by carbon ion implantation", PHYSICA STATUS SOLIDI-RAPID RESEARCH LETTERS 1 (6), 277-279 (2007)

[14] Zhao , Jin-Hua, Liu , Xiu-Hong, Huang , Qing, Liu, Peng, Wang Lei and Wang , Xue-Lin, “The array waveguides formed in LiNbO3 crystal by oxygen ion implantation”, Nuclear Instruments and Methods in Physics Research Section B: Beam Interactions with Materials and Atoms, 268, 2923–2925 (2010)

[15] Montanari, G. B., De Nicola, P. , Sugliani, S. , Menin, A., Parini, A., Nubile, A. Bellanca, G., Chiarini, M., Bianconi, M. , and Bentini, G. G., “Step-index optical waveguide produced by multistep ion implantation in LiNbO3”, Optics Express, 20, 4444 -4453 (2012)

[16] Ruiyun He, Shuqian Sun, Miaomiao Xu, Feng Chen, Shavkat Akhmadaliev, Shengqiang Zhou, “Planar optical waveguide in SrTiO3 crystal fabricated by carbon ion irradiation”, Nucl. Instr. and Meth. in Phys. Res. B, 308, 6-8 (2013)

[17] Liu Chun-Xiao; Xu Jun; Xu Xiao-Li; Wu Shu; Wei Wei; Guo Hai-Tao; Li Wei-Nan; and Peng Bo, Oxygen-implanted optical planar waveguides in Er^{3+}/Yb^{3+}-codoped silicate glasses for integrated laser generation, Optical Engineering, 53(3), 037101 (2014)

[18] Chen, Feng , Wang, Xue-Lin, Wang, Ke-Ming, Lu, Qing-Ming, and Shen, Ding-Yu, "Optical waveguides formed in Nd:YVO_4 by MeV Si^+ implantation", Appl. Phys. Lett, 80, 3473 (2002)

[19] Vázquez, G. V., Rickards, J., Lifante, G. , Domenech, M. and Cantelar, E., "Low dose carbon implanted waveguides in Nd:YAG", Optics Express, 11, 1291 - 6 (2003)

[20] Townsend, P. D., Chandler, P. J., Wood, R. A., Zhang, L., McCallu, J., and McHargue, C. W., "Chemically stabilised ion implanted waveguides in sapphire," Electron. Lett., 26, 1193-1194 (1990)

[21] Aithal, P. Sreeramana, Nagaraja, H. S., Mohan Rao, P, Avasthi, D. K., and Sarma, Asati, "Effect of high energy ion irradiation on electrical and optical properties of para-hydroxy acetophenone", Journal of Applied Physics 81, 7526 (1997); doi: 10.1063/1.365294

[22] Opfermann, Th., Höche, Klaumünzer, S., Wesch, W, "Formation of amorphous tracks in KTiOPO4 during swift heavy ion implantation", Nucl. Instr. and Meth. in Phys. Res. B, 166-167, 954-958 (2000)

[23] Gibbons, J.F., "Ion implantation in semiconductors—Part II: Damage production and annealing", Proceedings of the IEEE, 60, 1062 – 1096, (1972), DOI: 10.1109/PROC.1972.8854

[24] Bentini, G. G., Bianconi, M., Correa, L., Chiarini, M., Mazzoldi, P., C. Sada, N. Argiolas, Bazzan, M., and Guzzi, R., "Damage effects produced in the near-surface region of x-cut LiNbO3 by low dose, high energy implantation of nitrogen, oxygen, and fluorine ions", Journal of Applied Physics 96, 242-247 (2004)

[25] Olivares, J., García, G., Agulló-López, F., Agulló-Rueda, F., Kling, A., Soares, J.C., "Generation of amorphous surface layers in $LiNbO_3$ by ion-beam irradiation: thresholding and boundary propagation", Appl. Phys. A, 81, 1465–1469 (2005) DOI: 10.1007/s00339-005-3237-x

[26] Olivares, J., García, García-Navarro, Agulló-López, F., A., Caballero, O., García-Cabañes, A, "Generation of high-confinement step-like optical waveguides in $LiNbO_3$ by swift heavy ion-beam irradiation", Appl. Phys. Lett., 86, 183501 (2005)

[27] Bányász, I., Fried, M., Dücső, Cs., and Vértesy,Z., "Recording of transmission phase gratings in glass by ion implantation", Appl. Phys. Lett.,79, 3755 (2001)

[28] Berneschi, S., Nunzi Conti, G, Bányász, I., Watterich, A., Khanh, N. Q., Fried, M., Pászti, F., Brenci, M., Pelli, S., Righini, G. C., "Ion beam irradiated channel waveguides in Er^{3+}-doped tellurite glass", Appl. Phys. Lett., 90, 121136 (2007)

[29] Rajta, I, Szilasi, S.Z., Budai, J., Tóth, Z., Petrik, P., Baradács, E., "Refractive index depth profile in PMMA due to proton irradiation", Nucl. Instr. Meth. B, 260, 400-404 (2007)

[30] Bettiol, A.A., Udalagama, C.N.B., Teo, E.J., van Kan, J.A., Watt, F., "Embedded photonic structures fabricated in photosensitive glass using proton beam writing", Nucl. Instr. and Meth. B, 260, 357 (2007)

[31] Ziegler, J.F., "SRIM-2003", Nucl. Instr. and Meth.B, 219–220, 1027 (2004), and http://www.srim.org

[32] Olivares, J, Crespillo, M. L., Caballero-Calero, O, Ynsa, M.D., García-Cabañes, A., . Toulemonde, M., Trautmann, C., and Agulló-López, F., "Thick optical waveguides in lithium niobate induced by swift heavy ions (~10 MeV/amu) at ultralow fluences", Optics Express, 17, 24175 - 24182 (2009)

[33] Bányász, I., Berneschi, S., Fried, M., Lohner,T., G. Nunzi Conti, G.C, Righini, S. Pelli, Zolnai, Z., "M-line spectroscopic, spectroscopic ellipsometric and microscopic measurements of optical waveguides fabricated by MeV-energy N^+ ion irradiation for telecom applications", Thin Solid Films, 541, 3-8 (2013), doi: 10.1016/j.tsf.2012.11.134